Clinical and Experimental Pharmacology and Physiology (2009) **36**, 238–247

CEPP Frontiers in Research

Frontiers in Research Review:

New Frontiers in Biomedical Engineering

ENGINEERING IMAGING: USING PARTICLE IMAGE VELOCIMETRY TO SEE PHYSIOLOGY IN A NEW LIGHT

Andreas Fouras,*† Jonathan Dusting,‡ John Sheridan,† Masaaki Kawahashi,§ Hiroyuki Hirahara§ and Kerry Hourigan*†

**Division of Biological Engineering, †Fluids Laboratory for Aeronautical and Industrial Research (FLAIR), Department of Mechanical and Aerospace Engineering, Monash University, Melbourne, Victoria, Australia, ‡Division of Engineering, Kings College London, London, UK and §Department of Mechanical Engineering, Saitama University, Saitama, Japan*

SUMMARY

1. Despite the array of sophisticated imaging techniques available for biological applications, none of the standard biomedical techniques adequately provides the capability to measure motion and flow. Those techniques currently in use are particularly lacking in spatial and temporal resolution.

2. Herein, we introduce the technique of particle image velocimetry. This technique is a well-established tool in engineering research and industry. Particle image velocimetry is continuing to develop and has an increasing number of variants.

3. Three case studies are presented: (i) the use of microparticle image velocimetry to study flow generated by high-frequency oscillatory ventilation in a human airway model; (ii) the use of stereoparticle image velocimetry to study stirred cell and tissue culture devices; and (iii) a three-dimensional X-ray particle image velocimetry technique used to measure flow in an *in vitro* vascular flow model.

4. The case studies highlight the vast potential of applying the engineering technique of particle image velocimetry and its many variants to current research problems in physiology.

Key words: bioreactor, blood flow velocity, computer-assisted three-dimensional imaging, fluidics, lung ventilation, microfluidics, particle image velocimetry, rheology, tissue culture.

INTRODUCTION

As is well known, between 60 and 70% of the human body is comprised of fluids. A range of important fluid flows occur, such as blood flow, airflow in the respiratory tract, lymphatic flow and lubrication of synovial joints. Many of these flows are highly complex and have not been well quantified, thus limiting our understanding of the physiological systems in which they occur.

A wide range of imaging techniques is available for biological applications, including microscopy (bright-field, fluorescent, phase contrast and confocal), magnetic resonance imaging (MRI), radionuclide imaging, X-ray angiography, X-ray computed tomography (CT), X-ray videodensitometry, video cross-correlation tracking and ultrasonography. A review of all these techniques can be found in Fouras *et al.*[1] Of these techniques, X-ray videodensitometry and video cross-correlation tracking measure the total or average flow in a region, usually a blood vessel segment. These techniques have extremely poor spatial and temporal resolution and can only characterize flows as a single parameter rather than as a velocity field that may vary in space and time. This limitation becomes significant in many physiological flows (e.g. blood flow, for which there is variation during the cardiac cycle and across the vessel diameter). Magnetic resonance imaging and ultrasonography have the capability to resolve details of the flow, but are also limited in spatial and temporal resolution. Vennemann *et al.*[2] reported a spatial resolution of 0.1 mm for both ultrasound and MRI, but this is perhaps the best possible performance and is rarely achieved. Vennemann *et al.*[2] also noted that ultrasound and MRI have a measurement time of approximately 100 msec, but because MRI is almost always performed over many slices, it is often approximately 5 s before a repeat measurement can be performed. The technique known as particle image velocimetry (PIV) can also be used to measure fluid flows, but with a vastly higher resolution, typically of the order of microns.

"capability to measure motion and flow"

Correspondence: Andreas Fouras, Division of Biological Engineering, Monash University, Melbourne, Victoria 3800, Australia. Email: fouras@eng.monash.edu. This paper has been peer reviewed. Received 19 April 2008; revision 28 August 2008; accepted 16 September 2008.

doi: 10.1111/j.1440-1681.2008.05102.x

Frontiers in Research

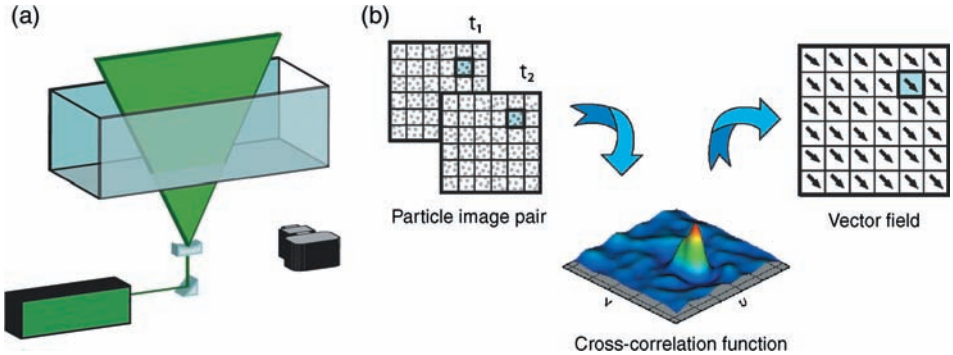

Fig. 1 Schematic diagrams showing generic implementations of (a) the laser illumination and imaging of standard two-dimensional particle image velocimetry (PIV) and (b) PIV cross-correlation analysis. The analysis involves subdividing each pair of images into a grid-like set of sampling windows and performing a cross-correlation between corresponding sampling windows in each frame. The peak in each correlation relates to the velocity at each grid location.

PARTICLE IMAGE VELOCIMETRY

At present, PIV is the most commonly used technique to measure velocity fields and derived properties, such as shear, in the engineering disciplines. The technique finds use in the full spectrum of fluid mechanics experiments, from water and wind tunnel measurements for aerodynamics, water channel studies for off-shore and marine studies, to microchannels that sit on a microscope slide for microfluidics studies.

Schematic representations of PIV imaging and analysis are shown in Fig. 1a,b. As the name suggests, PIV is an image-based technique. Typically, laser light is used to illuminate the region of interest, which includes fluid seeded with reflective tracer particles. These particles are usually close to neutrally buoyant in order to adequately describe the flow (Fig. 1a). Pairs of images separated by a known time interval are typically captured using a charge-coupled device (CCD) camera, which is synchronized with the laser. The time interval used is highly dependent on the magnification and nature of the flow, but is often less than 1 msec. To allow images to be taken at very short time intervals, specialized cameras have been developed that acquire images in pairs rather than continuous sequences.

"velocity at each grid location"

In its most basic form, PIV analysis involves subdividing each image into a grid-like set of sampling windows and performing a cross-correlation analysis between corresponding sampling windows in each frame. As shown in Fig. 1b, the cross-correlation analysis is conducted at every sampling window location on the grid. The peak of each cross-correlation represents the most common particle displacement inside the volume imaged in that sampling window. The instantaneous velocity at each grid location is then simply the ratio of the measured displacement and the time separation between images. A review of the advances over the past 20 years in the field of PIV can be found elsewhere.[3]

Since its inception, PIV has been under continuous development and improvement. Newer PIV variants include stereoscopic PIV techniques,[4–6] which allow for three-component velocity vector measurements over a plane, and holographic PIV techniques,[7,8] which allow three-dimensional measurements to be made over a volume. More recently, micro PIV[9,10] (μPIV) has been developed and has been used extensively because it allows measurements to be performed on microfluidic devices. Over time, engineers have found an increasing number of biological applications for PIV techniques.

The optical nature of PIV is the source of its greatest strengths and limitations. The technique allows simultaneous measurements over the area of a field of view, but requires visibility of that area to perform those measurements. This can be particularly limiting in *in vivo* studies, where direct optical visualization is often not available. However, many physiologically important models that allow optical access have been developed. These include models such as embryos and small animals (e.g. zebrafish), as well as important *in vitro* models. Examples of PIV application to biological research include the use of PIV to measure blood flow profiles in surgically exposed mesenteric vessels of rats[11,12] and the measurement of blood flow velocity within an embryonic avian heart.[13] The aim of the present paper is to introduce biologists to further possibilities of PIV application.

CASE STUDIES IN THE APPLICATION OF PIV TO PHYSIOLOGY

In this paper, three case studies of the application of PIV to physiologically relevant fluid flows are presented, each illustrating a different biological application and PIV configuration. The first case study highlights research undertaken to uncover a key component of the fluid mechanics of high-frequency oscillatory ventilation (HFOV). The phenomenon under investigation is the pendelluft flow, whereby gas flows back and forth between alveoli in a

manner similar to a pendulum. This phenomenon was studied using an implementation of μPIV.

The next case study is of the fluid flow within a tissue or cell culture device, commonly known as a stirred bioreactor. Owing to the highly three-dimensional nature of this flow, stereo PIV (SPIV) was used because it provides all three components of velocity on the plane being investigated. Stereo PIV uses two (or more) imaging systems in combination to measure the flow, consequently capturing the out-of-plane components that single imaging systems cannot measure and that are crucial in such stirred flows.

The third and final case study uses a new X-ray PIV technique to measure velocities in an *in vitro* model of vascular flow. This technique uses the penetrating powers of X-rays and has the potential to measure flow deep inside tissue and living animal models and can resolve velocity data at the scale of blood elements or better.

Case study 1: Investigation of pendelluft flow generated by HFOV in a human airway model

Introduction

Many artificial respiration methods have been applied as clinical procedures for patients with respiratory disorders. In diseased lungs, positive pressure ventilation may not always provide adequate gas exchange and may even result in tissue damage owing to ventilating at high airway pressures.[14] High-frequency oscillatory ventilation uses a low tidal volume and a high frequency to allow CO_2 clearance and O_2 delivery without risks associated with high airway pressure. High-frequency oscillatory ventilation has been noted as an effective technique for the medical care of pulmonary disease patients, especially infants.[15–17] Many studies of respiratory flow in a bifurcating airway model by HFOV have been performed both experimentally and theoretically. Chang[18] and Krishnan and Brower[19] presented several mechanisms of gas exchange during ventilation by high-frequency oscillation, including six mechanisms of gas mixing during HFOV. One of these is pendelluft flow, defined as gas exchange between parallel respiratory units with different time constants. Pendelluft flow is an important factor in gas exchange during HFOV. Although many studies have focused on the effect of treatment using HFOV, the pendelluft gas transport mechanisms, in the terminal airways of the human lung, have not been measured or explained in detail.

"resolve velocity data at the scale of blood elements"

This case study is based on the first step of an investigation of pendelluft flow in the terminal airways during HFOV. The details of the study can also be found in Lee *et al*.[20] A single, symmetric bifurcation with different daughter branch volumes, modelled on an 18th- and 19th-generation bronchial tube, was used to measure the pendelluft flow during HFOV. The gas velocity of pendelluft and oscillatory flow in the model bronchial tubes was measured using μPIV.

Methods

The terminal airways have very small dimensions, so it is difficult to model and analyse the entire peripheral airway in the lung. For simplicity, a Y-shaped bifurcation with two generations (i.e. a set of one parent and two daughter bronchial tubes) is adopted. The configuration is symmetric and its dimensions are full scale. The geometry was determined to be of similar order as the basic anatomical features of the human terminal airway bifurcation.[21]

A schematic diagram of the experimental apparatus is shown in Fig. 2. The test channel is made of an aluminium plate of 500 μm thickness and has dimensions corresponding to an 18th–19th-generation bronchiole. The channels were precisely machined with the dimensions described in Lee *et al*.[20] and processed with a black alumite coating in order to reduce the reflection of the laser light. The microchannel was mounted between glass plates to allow

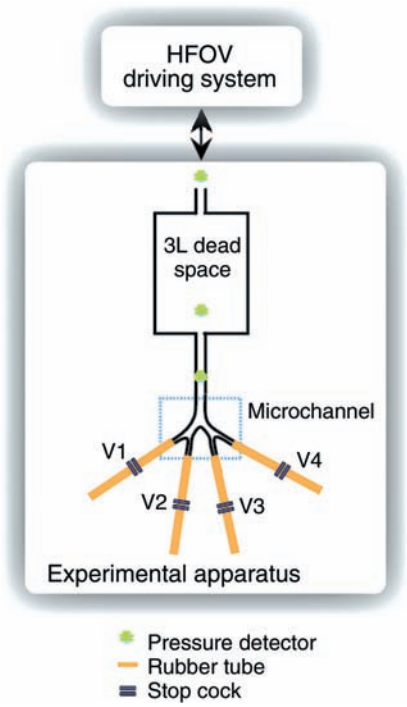

Fig. 2 Schematic diagram of experimental apparatus showing a high-frequency oscillatory ventilation (HFOV) system, measurement apparatus and a microchannel test section in which micro particle image velocimetry experiments where performed.

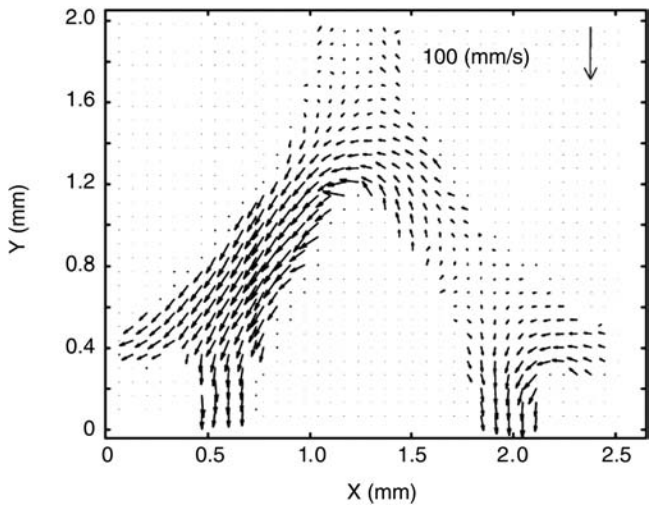

Fig. 3 Instantaneous velocity vectors, showing multiple pendelluft motions for the case of volume ratios of 4 : 4 : 4 : 2.

observation. In this study, the oscillatory flow was driven by an oscillating piston. In order to model the effects of the upper parts of the lung on the modelled section, a 3 L chamber was installed between the HFOV system and the microchannel. The entire system was monitored using three pressure sensors.

Accurate modelling of a real lung is quite difficult. To examine the pendelluft movement in this model, the effects of different compliance and resistance were substituted by changing the length of the rubber tubes, as shown in Fig. 2. The rubber tubes were connected to the end of each daughter branch. Air volumes and compliances in each rubber tube can be adjusted by pinching the tube to a shorter length.

The test section was illuminated by a diode laser and images were captured using a high-speed camera through a microscope objective lens. Smoke generated by burning incense was used as tracer particles with a nominal diameter of 0.5 μm. Decades of engineering experiments have demonstrated that smoke very accurately follows the flow of gas, making it an excellent tracer. The smoke was introduced by charging it into the dead-space chamber before each experiment. The flow rate was maintained at 8 L/min with a low-pass filter and HFOV parameters at a stroke volume and frequency of 30 mL and 15 Hz, respectively.

Results and Discussion

Results from the μPIV measurements are shown in Fig. 3. The data in Fig. 3 are velocity vectors. These vector arrows show the direction and magnitude of the flow (compared with the reference vector in the upper right) at the end of inspiration and expiration, respectively, for the case of a volume ratio of 4 : 4 : 4 : 1.

In the respiratory units, with high compliance and resistance, the gas fills the volume slowly; that is, it has a long time constant. Conversely, units with a low compliance and resistance have a short time constant: the gas fills the volume quickly. This morphology results in a phase delay in inspiration or expiration for low-frequency (normal) breathing cycles but, in the case of HFOV, results in pendelluft flow. Furthermore, the intensity and duration of pendelluft flow in the airway model is found to be strongly dependent on the unequal volume of branches, which also corresponds to the difference of time constant.

This difference of time constant can be clearly seen in Fig. 3. The right-hand element (with a lower volume and hence lower time constant) fills first, resulting in flow from this element into the parallel element (second from the right). Also note that, in total, the two elements on the right have less volume than the two elements on the left, also resulting in flow at this generation, from right to left. Finally, note that the flow is equally shared between the two left-hand elements because they have the same time constant (compliance).

The feasibility and usefulness of μPIV for the experimental analysis in this research field have been validated. Measurement techniques with a poor temporal resolution (including MRI, ultrasound, X-ray videodensitometry and video tracking cross-correlation) are unlikely to measure any pendelluft flow at all, because the velocities measured by these techniques would be averaged over many ventilation cycles, resulting in a velocity reading of zero. Visualization and measurement of the pendelluft effect generated by HFOV in the double bronchial bifurcation model have been established using μPIV. In order to explain gas transport, additional geometries with realistic compliance and resistance will need to be used to clarify the complicated phenomena associated with pendelluft flow in bronchial respiration. Micro PIV is the tool of choice for measurements in these physiologically important *in vitro* models. For *in vivo* models, techniques such as that outlined in case study 3 show great potential.

"Improving the outcomes of cell and tissue culture"

Case study 2: Optimizing bioreactor design for cell and tissue culture using SPIV

Introduction

Improving the outcomes of cell and tissue culture through the use of bioreactors is a goal that has recently received substantial research interest, as illustrated, for example, by the 146 papers discussed in the recent reviews by Darling and Athanasiou[22] and Martin *et al.*[23]

This interest has been generated, in part, by strong advancements in the fields of tissue engineering and cell culture-based research. In particular, there is now the need to produce therapeutically relevant cell yields or tissue constructs on a scale that goes far beyond what is typically required for laboratory use.[23–25] Several studies have attempted to use existing knowledge of the way in which physiological flows affect cell growth to propose suitable *in vitro* cell culture devices, or bioreactors, for particular cell or tissue culture applications.

Popular bioreactor types include spinner-flasks,[26,27] rotating wall bioreactors,[28–32] perfusion reactors[33–36] and shaking bioreactors. Martin *et al*.[23] summarized various types of bioreactors used for tissue engineering applications. Thouas *et al*.[37] describe the use of bioreactors to model tumour progression.

Most of the bioreactors described in the literature were selected without undertaking a detailed consideration of the fluid dynamic conditions within them, despite the fact that the local shear stresses are known to be crucial to the functional growth of many important mammalian cell types, including endothelial cells,[38] osteoblasts,[39] neural stem cells[40] and chondrocytes.[41] The most suitable bioreactor configuration for a particular phenotype will depend on the required oxygen and nutrient supply, culture medium and local stress levels. Bioreactor flow properties that can influence in vitro culture include the shear stress magnitude and spatial distribution, mixing properties, temporal variability and turbulence levels.

"used engineering techniques of laser visualization"

Dusting *et al*.[42] used engineering techniques of laser visualization and PIV to characterize, in detail, a family of controlled flows that are scaleable and easily implemented within cylindrical vessels with a rotating bottom and a free surface. The authors demonstrated how a thorough characterization of a flow could be used to design or select bioreactors that will be optimized appropriately for different cell or tissue culture applications. This second case study is based on that work.

The chosen vessel configuration is that of a vertically orientated cylindrical chamber with a rotating bottom, of diameter matching the cylinder and a free surface. The primary reason this geometry has been selected is that it has the simplicity of the spinner flask, without the overly complex turbulent flow that results under typical user conditions.[43] Having control over the flow ensures repeatability of the hydrodynamic conditions to which cells are exposed.

Stereo PIV has been used to measure dynamic properties especially relevant to cell culture, in particular the velocity field in the secondary flow plane and the three-dimensional stress field. It is only with three-dimensional measurement techniques that these properties can be adequately quantified for this flow. As mentioned by Humphrey,[44] the quantification of stresses relevant to cell mechanics in terms of three-dimensional stresses is highly preferable to the more common practice of characterizing stress fields by the measurement of two-dimensional shear or, broader still, by a single global parameter.[45]

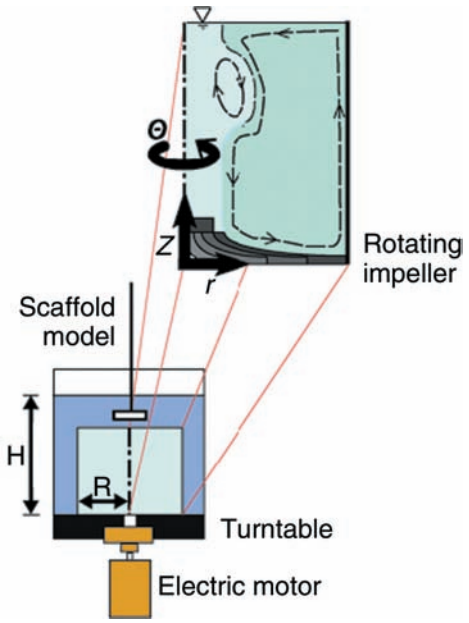

Fig. 4 Annotated rig vertical cross-section, with scaffold placement system, coordinate system and relevant dimensions. The inset shows the vortex breakdown flow pattern in the meridional plane. The two separate flow regions are shaded differently.

Methods

The experimental model (Fig. 4) consisted of a polished transparent container with a 65 mm diameter drilled centre hole, mounted onto a stainless steel base. The exterior faces of the block were kept flat in order to reduce optical distortion during the use of image-based measurement techniques. The scale was kept similar to that of mammalian cell bioreactor devices found in the literature, which typically have a fluid volume of approximately 100–300 mL. The top surface was left open during experiments as would be necessary to allow metabolic gas exchange during cell culture. A flat, circular disk acted as the rotating bottom and was fastened to a drive-shaft assembly that was located in the centre of the base, as illustrated in Fig. 4. The shaft was rotated by a computer-controlled stepper motor.

The coordinate system is illustrated in Fig. 4. The axes are defined cylindrically; that is, by radial (r), axial (z) and angular (y) positions. The origin corresponds to the top centre of the rotating disk. Positional data were typically normalized by cylinder radius, R, in the radial direction and surface height, H, in the axial direction. The

ratio H/R was kept constant at 1.5; however, a more optimal height ratio may be located by conducting additional characterizations. As a comparison, Vunjak-Novakovic *et al.*[45] used H/R = 1.05 and Sucosky *et al.*[43] used H/R = 1.17.

The experimental scaffold models consisted of a disk and a supporting column. The disks were cylindrical in shape with a circular cross-section. The disk aspect ratio, thickness/radius, was held at 0.40. In order to investigate the effect of varying the scaffold to bioreactor radius ratio, three disks were used. The radius of the smallest disk was 2.5 mm and the dimensions of the other disks were multiples of this (5.0 and 7.5 mm). Therefore, the radius ratios investigated were 1/13, 2/13 and 3/13.

Stereo PIV was the primary tool used for quantitative flow measurement. The stereoscopic technique is an extension of traditional PIV, which uses two (or more) imaging systems in combination to measure the flow, including the out-of-plane components that single imaging systems cannot measure.

The necessity in this study to measure all three velocity components arises mainly for two reasons. First, the high ratio of out-of-plane to in-plane velocity components in the measurement plane caused a relatively high perspective error in two-dimensional PIV studies. Second, the capability to measure the third component of velocity added significant detail to the results. This was especially relevant to the present study, because one aim was to gain as much information as possible about the stresses acting within the fluid and along scaffold surfaces.

"This shear borders … as vortex breakdown"

The setup used two CCD cameras at right angles, with each having an image resolution of 1360 × 1024 pixels. In this case, a measurement resolution of 96 × 50 vectors was enabled. The spacing between vectors obtainable using SPIV was 0.02R. The stress fields derived using SPIV were validated by comparing them with stress fields derived by computer simulation. The SPIV technique used in this case study very closely follows Fouras *et al.*[46]

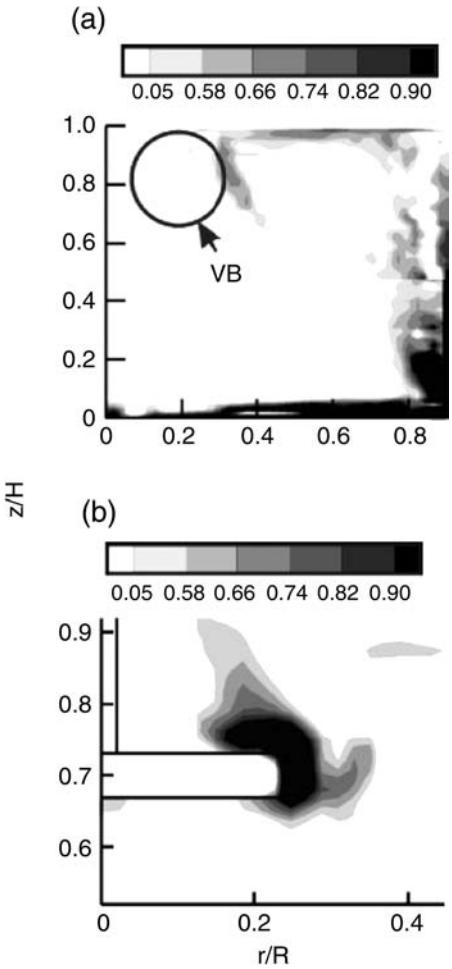

Fig. 5 (a) Bioreactor at moderate disc rotation rate in cell suspension mode (without tissue scaffold) showing magnitude of shear stress with the location of the vortex breakdown (VB) marked with circle; (b) Bioreactor at moderate disc rotation rate in tissue culture mode (with tissue scaffold of size r/R = 3/13, located at z/H = 0.7), showing magnitude of shear stress in the vicinity of the tissue scaffold.

Results and Discussion

Figure 5 shows a sample of key results from this study. Figure 5a shows results for a moderate rate of rotation for the case of a cell suspension bioreactor (no cell scaffold). This figure shows the magnitude of the shear stress across the entire domain of the bioreactor. Towards the top of the figure, a region of high shear can be seen. This shear borders on a phenomenon termed by engineers as vortex breakdown (VB), a bubble of recirculating fluid. It can be seen that although the shear stress on the edge of the VB is high, it is very low inside the VB.

Figure 5b illustrates results for a moderate rate of rotation for the case of a tissue engineering bioreactor (including cell scaffold), showing the magnitude of the shear stress in the immediate vicinity of the bioreactor. The maximal shear stress occurs on the radial periphery of the scaffold.

For freely suspended cell or microcarrier culture, flows at disk rotation rates below that for the onset of VB may not have the momentum to provide adequate mixing or to suspend the cell aggregates for long periods of time. As the rate of rotation increases, the disk rotation becomes sufficient to cause circulation through the axial and meridional planes. Above a certain threshold, the on-axis VB bubble appears on the central axis, albeit small at first. With an

increase in rotation rate, both the size and geometry of this region change. It appears possible, when considering the entrainment of particles in the VB region during flow visualization, that this region may provide suitable conditions for cell culture. The VB region may be considered a virtual reactor with nutrients and waste passing between the VB and the rest of bioreactor, but with the VB region isolated from the damaging regions of strong shear that may be present in the remainder of the fluid volume.

"will only be of real use for bioreactor design"

This study provides an introductory demonstration of how PIV may be used to quantify flows for cell culture applications. The SPIV techniques were used to study the flow and shear under conditions representative of freely suspended cell culture and stationary–suspended scaffold/bioreactor systems.

The dearth of knowledge regarding how cells respond to stresses is currently being addressed by researchers in many different fields of cellular engineering and will only be of real use for bioreactor design when used in combination with techniques such as these.

Case study 3: Measurement of vascular flow using three-dimensional, X-ray PIV

Introduction

Vascular disease is the leading cause of morbidity and mortality in the developed world. Due to our ageing population, the burden of this disease is expected to continue to grow over coming decades. There is an increasing appreciation of the importance of vascular fluid dynamics, shear and rheology in the genesis of vascular disease. However, the details of the relationship between properties of vascular flow and the processes of vascular disease remain ill-defined. One of the key barriers to the progression of our understanding of these factors is the inability to make detailed measurements of vascular flow in any but the thinnest or most transparent of vessels.

It is difficult to measure vascular flow in any but the thinnest vessels. As discussed previously, medical imaging techniques that have been used previously to measure flows *in vivo*, such as ultrasonography and MRI, are generally restricted to velocity field measurements with spatial resolutions of millimetre precision. The PIV techniques, which are known to measure velocity data with resolution of blood elements or better, are restricted by a lack of optical access. An exciting idea is the combination of high-resolution image-processing techniques and X-ray imaging with its unparalleled resolution and excellent tissue penetration.

Seeger *et al.*[47] tracked individual particles in a bubble column in three-dimensional space using dual X-ray detector systems. However, in general, tracking individual particles results in significantly lower levels of information recording than statistical cross-correlation methods. Lee and Kim[48] subsequently used PIV rather than particle tracking and achieved far greater resolution. However, using an X-ray light source to conduct PIV poses its own significant problems, especially due to the fact that when the fluid region is volume illuminated, particle images will be smeared by the motion captured by the pseudo-continuous illumination.

Fouras *et al.*[49] developed a technique that solves these problems. In that paper, the authors greatly refine the techniques used previously to undertake velocity measurements with an X-ray light source, substantially enhancing accuracy (see Fig. 6b). Furthermore, an advanced cross-correlation peak analysis was developed to allow three-dimensional measurement of the velocity field.

Methods

This technique is simple to implement and means that, in future, X-ray PIV practitioners will be able to achieve simple two-dimensional measurements with a synchrotron light source. Although flows in a number of different vascular models have been measured using this technique, including *intra vital* flows, we report here on the study in an *in vitro* vascular flow model. The *in vitro* flow model consisted of a 15 mm diameter pipe filled with glycerin and containing silver-coated hollow glass microspheres. The glycerin was pumped through the pipe using a syringe pump. The experiments were conducted at the SPring8 synchrotron with the approval of the Japan Synchrotron Radiation Research Institute (JASRI). The experiments were conducted on the biomedical beam-line (20B2) with a 25 keV X-ray beam that was approximately 25 mm in height and 40 mm in width. The images were acquired with a Hamamatsu beam monitor (BM4; Hamamatsu Photonics, Hamamatsu, Japan) with 4000 × 2642 pixels and a pixel size of 5.87 μm. Figure 6a shows the basic layout of the experiment and coordinate system.

Results and Discussion

For a more quantitative evaluation of the technique, the calculated maximum flow profile is compared with the measured profile in Fig. 6b. For completeness, the measured profile using the published technique of Lee *et al.*[20] is also shown. The excellent agreement between the measured maximum velocity and the theoretical value is clear.

The correlation peak contains velocity information about the entire measurement volume. With some additional mathematics and some minor assumptions, the velocity profile was calculated at each (x, y, z) position inside the pipe over a sequence of 40 frame pairs. These velocities were averaged over time and then plotted as a function of y and z at three different x locations, as shown in Fig. 6c. The velocity field cross-section is close to the expected profile (known as the Poiseuille flow profile), with little variation at different x locations. The coloured contour shading included in Fig. 6c helps illustrate the similarity at each x location. The successful derivation

Frontiers in Research

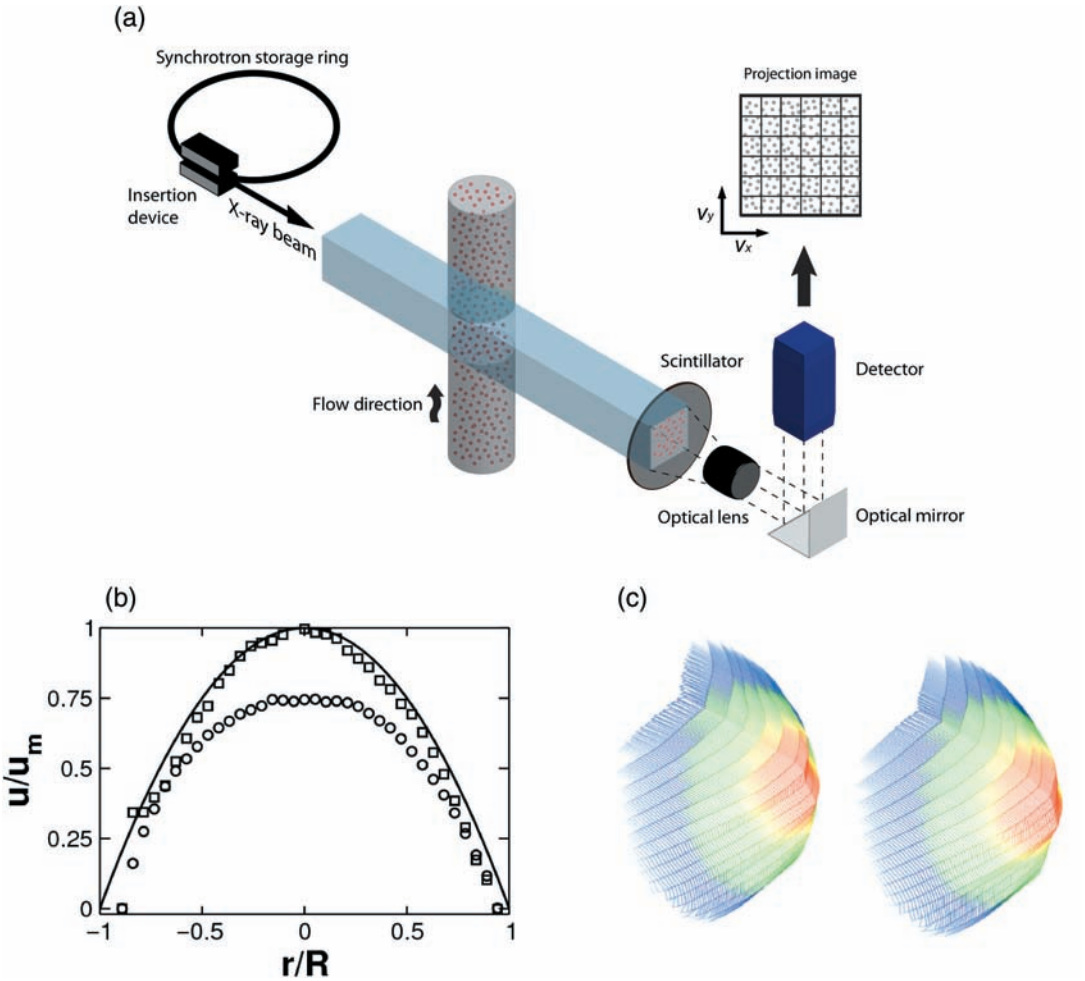

Fig. 6 (a) Schematic of the synchrotron X-ray particle image velocimetry (PIV) and pipe flow system, as well as the coordinate system. Experiments were performed at SPring8 BL 20B2 at 25 keV with a beam of 25 mm height and 40 mm width. (b) Measured average velocity profile based on different cross-correlation peaks: squares represent final measured velocities; circles represent velocities measured using techniques outlined in Lee *et al.*;[48] the solid line represents the theoretical (expected) velocity profile. (c) Reconstructed three-dimensional velocity field inside a round pipe. Every node on the mesh corresponds to a different measured value. The coloured contours represent the magnitude of velocity.

of the three-dimensional Poiseuille flow validates the accuracy of the technique.

In this case study, a new X-ray PIV technique has been used successfully to measure flow in an *in vitro* vascular flow model. Although an idealized model was used here to validate the acquired flow, the technique could be applied to measure more useful physiological cases of *intra vital* or even *in vivo* flows. The authors have successfully achieved measurements of blood flow, where erythrocytes themselves have been used as the tracer particle.

"erythrocytes themselves have been used as the tracer particle"

The authors further anticipate that, in the future, the measurement of vasculature from multiple perspectives will be possible, combining the advantages of both SPIV and X-ray CT. Such measurements will have the powerful combinations of high resolution and excellent tissue penetration, as well as fully three-dimensional measurements of both form and function.

CONCLUSIONS

The technique of PIV has been introduced. Particle image velocimetry is undergoing a constant process of review and development. Applications continue to grow in the discipline of Engineering, but

Frontiers in Research

many engineers are seeking to adapt and modify PIV for application in Physiology and Biomedicine in general. Three case studies of the application of PIV to research problems in physiology were presented.

A case study of the use of μPIV to study flow generated by HFOV in a human airway model was presented. In this study, the fundamental characteristics of pendelluft flow generated by HFOV in a bronchiole duct model with different branch volume ratios were established by using the μPIV technique. The pendelluft flow was clearly observed and its nature and shape were fully quantified using μPIV. It is asserted that no other technique available at this time has both the spatial and temporal resolution to make these kinds of measurements. These measurements of *in vitro* models can aid our understanding of the mechanisms of phenomena (such as CO_2 clearance), potentially leading to important results, such as the development of new ventilation strategies.

"PIV techniques in the biological sciences continues to expand"

A case study of the use of SPIV for a project to optimize stirred cell and tissue culture devices was also presented. Stereo PIV techniques were successfully used to study the flow under conditions representative of freely suspended cell culture and stationary–suspended scaffold/bioreactor systems. In this case, velocity data were accompanied by shear data calculated from the velocity data. This study provides an introductory demonstration of how PIV may be used to quantify flows for cell culture and other laboratory applications.

The third and final case study presented in this paper was of an X-ray particle image velocimetry technique used to measure the flow in an idealized *in vitro* vascular flow model. In this study, the viability of X-ray PIV has been demonstrated and it is proposed that this technique could be used for three-dimensional measurement of *in vivo*, *intra vital* or *in vivo* flow.

Current obstacles to widespread implementation of PIV for biological flow measurement applications include the need for optical access and the requirement of flow seeding with tracer particles. For many *in vivo* applications, appropriate X-ray imaging or seeding may not be available. In these cases, a model is usually required, which may potentially reduce the physiological relevance of the measurements. However, in many cases, generalized flow measurements acquired *in vitro* help provide an understanding of physiologically relevant properties, such as the shear stresses or mass transport within vessels, or the flow-dependence of biological materials, such as cells, tissue, DNA or proteins. For this reason, the application of PIV techniques in the biological sciences continues to expand.

REFERENCES

1. Fouras A, Kitchen MJ, Dubsky S, Lewis RA, Hooper SB, Hourigan K. The past, present and future of X-ray technology for *in vivo* imaging of form and function. *J. Appl. Phys*. 2009 (in press).
2. Vennemann P, Lindken R, Westerweel J. *In vivo* whole-field blood velocity measurement techniques. *Exp. Fluids* 2007; **42**: 495–511.
3. Adrian RJ. Twenty years of particle image velocimetry. *Exp. Fluids* 2005; **39**: 159–69.
4. Arroyo MP, Greated CA. Stereoscopic particle image velocimetry. *Meas. Sci. Technol*. 1991; **2**: 1181–6.
5. Fouras A, Lo Jacono D, Hourigan K. Target-free Stereo PIV: A novel technique with inherent error estimation and improved accuracy. *Exp. Fluids* 2008; **44**: 317–29.
6. Willert C. Stereoscopic digital particle image velocimetry for application in wind tunnel flows. *Meas. Sci. Technol*. 1997; **8**: 1465–79.
7. Pu Y, Meng H. An advanced off-axis holographic particle image velocimetry (HPIV) system. *Exp. Fluids* 2000; **29**: 184–97.
8. Zhang J, Tao B, Katz J. Turbulent flow measurement in a square duct with hybrid holographic PIV. *Exp. Fluids* 1997; **23**: 373–81.
9. Olsen MG, Adrian RJ. Out-of-focus effects on particle image visibility and correlation in microscopic particle image velocimetry. *Exp. Fluids* 2000; **29**: S166–74.
10. Santiago JG, Wereley ST, Meinhart CD, Beebe DJ, Adrian RJ. A particle image velocimetry system for microfluidics. *Exp. Fluids* 1998; **25**: 316–19.
11. Sugii Y, Nishio S, Okamoto K. *In vivo* PIV measurement of red blood cell velocity field in microvessels considering mesentery motion. *Physiol. Meas*. 2002; **23**: 403–16.
12. Tsukada K, Minamitani H, Sekizuka E, Oshio C. Image correlation method for measuring blood flow velocity in microcirculation: Correlation 'window' simulation and *in vivo* image analysis. *Physiol. Meas*. 2000; **21**: 459–71.
13. Vennemann P, Kiger KT, Lindken R *et al*. *In vivo* micro particle image velocimetry measurements of blood-plasma in the embryonic avian heart. *J. Biomech*. 2006; **39**: 1191–200.
14. Brower RG, Matthay MA, Morris A *et al*. Ventilation with lower tidal volumes as compared with traditional tidal volumes for acute lung injury and the acute respiratory distress syndrome. *N. Engl. J. Med*. 2000; **342**: 1301–8.
15. Bohn DJ, Miyasaka K, Marchak BE, Thompson WK, Froese AB, Bryan AC. Ventilation by high-frequency oscillation. *J. Appl. Physiol*. 1980; **48**: 710–16.
16. Drazen JM, Kamm RD, Slutsky AS. High-frequency ventilation. *Physiol. Rev*. 1984; **64**: 505–43.
17. Leipala JA, Iwasaki S, Lee S, Milner AD, Greenough A. Compliance and resistance levels and unloading in proportional assist ventilation. *Physiol. Meas*. 2005; **26**: 281–92.
18. Chang HK. Mechanisms of gas-transport during ventilation by high-frequency oscillation. *J. Appl. Physiol*. 1984; **56**: 553–63.
19. Krishnan JA, Brower RG. High-frequency ventilation and the prevention of ventilator-associated lung injury. *Chest* 2001; **119**: 1978–9.
20. Lee WJ, Kawahashi M, Hirahara H. Experimental analysis of pendelluft flow generated by HFOV in a human airway model. *Physiol. Meas*. 2006; **27**: 661–74.
21. Weibel ER. Principles and methods for morphometric study of lung and other organs. *Lab. Invest*. 1963; **12**: 131–52.
22. Darling EM, Athanasiou KA. Articular cartilage bioreactors and bioprocesses. *Tissue Eng*. 2003; **9**: 9–26.
23. Martin I, Wendt D, Heberer M. The role of bioreactors in tissue engineering. *Trends Biotechnol*. 2004; **22**: 80–6.
24. Carrier RL, Papadaki M, Rupnick M *et al*. Cardiac tissue engineering:

Frontiers in Research

Cell seeding, cultivation parameters, and tissue construct characterization. *Biotechnol. Bioeng*. 1999; **64**: 580–9.
25. Wu F, Dunkelman N, Peterson A, Davisson T, De la Torre R, Jain D. Bioreactor development for tissue-engineered cartilage. *Ann. N.Y. Acad. Sci*. 1999; **875**: 405–11.
26. Cherry RS, Papoutsakis ET. Hydrodynamic effects on cells in agitated tissue-culture reactors. *Bioprocess Eng*. 1986; **1**: 29–41.
27. Leckie F, Scragg AH, Cliffe KC. Effect of bioreactor design and agitator speed on the growth and alkaloid accumulation by cultures of *Catharanthus roseus*. *Enzyme Microb. Technol*. 1991; **13**: 296–305.
28. Begley CM, Kleis SJ. The fluid dynamic and shear environment in the NASA/JSC rotating-wall perfused-vessel bioreactor. *Biotechnol. Bioeng*. 2000; **70**: 32–40.
29. Begley CM, Kleis SJ. RWPV bioreactor mass transport: Earth-based and in microgravity. *Biotechnol. Bioeng*. 2002; **80**: 465–76.
30. Freed LE, Vunjaknovakovic G. Cultivation of cell–polymer tissue constructs in simulated microgravity. *Biotechnol. Bioeng*. 1995; **46**: 306–13.
31. Goodwin TJ, Prewett TL, Wolf DA, Spaulding GF. Reduced shear-stress: A major component in the ability of mammalian-tissues to form 3-dimensional assemblies in simulated microgravity. *J. Cell. Biochem*. 1993; **51**: 301–11.
32. Kleis SJ, Schreck S, Nerem RM. A viscous pump bioreactor. *Biotechnol. Bioeng*. 1990; **36**: 771–7.
33. Nielsen LK. Bioreactors for hematopoietic cell culture. *Annu. Rev. Biomed. Eng*. 1999; **1**: 129–52.
34. Niklason LE, Gao J, Abbott WM *et al*. Functional arteries grown *in vitro*. *Science* 1999; **284**: 489–93.
35. Planchamp C, Vu TL, Mayer JM, Reist M, Testa B. Hepatocyte hollow-fibre bioreactors: Design, set-up, validation and applications. *J. Pharm. Pharmacol*. 2003; **55**: 1181–98.
36. Sodian R, Lemke T, Fritsche C *et al*. Tissue-engineering bioreactors: A new combined cell-seeding and perfusion system for vascular tissue engineering. *Tissue Eng*. 2002; **8**: 863–70.
37. Thouas GA, Sheridan J, Hourigan K. A bioreactor model of mouse tumor progression. *J. Biomed. Biotechnol*. 2007; **2007**: 32754.
38. Tarbell JM. Mass transport in arteries and the localization of atherosclerosis. *Annu. Rev. Biomed. Eng*. 2003; **5**: 79–118.
39. Tate MLK. 'Whither flows the fluid in bone?' An osteocyte's perspective. *J. Biomech*. 2003; **36**: 1409–24.
40. Sen A, Kallos MS, Behie LA. Effects of hydrodynamics on cultures of mammalian neural stem cell aggregates in suspension bioreactors. *Ind. Eng. Chem. Res*. 2001; **40**: 5350–7.
41. Smith RL, Donlon BS, Gupta MK *et al*. Effects of fluid-induced shear on articular chondrocyte morphology and metabolism *in vitro*. *J. Orthop. Res*. 1995; **13**: 824–31.
42. Dusting J, Sheridan J, Hourigan K. A fluid dynamics approach to bioreactor design for cell and tissue culture. *Biotechnol. Bioeng*. 2006; **94**: 1196–208.
43. Sucosky P, Osorio DF, Brown JB, Neitzel GP. Fluid mechanics of a spinner-flask bioreactor. *Biotechnol. Bioeng*. 2004; **85**: 34–46.
44. Humphrey JD. Stress, strain, and mechanotransduction in cells. *J. Biomech. Eng. Trans. ASME* 2001; **123**: 638–41.
45. Vunjak-Novakovic G, Freed LE, Biron RJ, Langer R. Effects of mixing on the composition and morphology of tissue-engineered cartilage. *AIChE J*. 1996; **42**: 850–60.
46. Fouras A, Dusting J, Hourigan K. A simple calibration technique for stereoscopic particle image velocimetry. *Exp. Fluids* 2007; **42**: 799–810.
47. Seeger A, Affeld K, Goubergrits L, Kertzscher U, Wellnhofer E. X-Ray-based assessment of the three-dimensional velocity of the liquid phase in a bubble column. *Exp. Fluids* 2001; **31**: 193–201.
48. Lee SJ, Kim GB. X-Ray particle image velocimetry for measuring quantitative flow information inside opaque objects. *J. Appl. Physiol*. 2003; **94**: 3620–3.
49. Fouras A, Dusting J, Lewis R, Hourigan K. Three-dimensional synchrotron X-ray particle image velocimetry. *J. Appl. Phys*. 2007; **102**: 064916 1–6.